# MiFi: Device-free Wheat Mildew Detection Using Off-the-shelf WiFi Devices

<sup>†</sup>Pengming Hu, <sup>†</sup>Weidong Yang, <sup>‡</sup>Xuyu Wang, and <sup>§</sup>Shiwen Mao <sup>†</sup>College of Information Science and Engineering, Henan University of Technology, Zhengzhou, Henan, P.R. China 450066 <sup>‡</sup>Department of Computer Science, California State University, Sacramento, CA 95819-6021, USA <sup>§</sup>Department of Electrical and Computer Engineering, Auburn University, Auburn, AL 36849-5201, USA Email: huhelai007@163.com, Yangweidong@haut.edu.cn, xuyu.wang@csus.edu, smao@ieee.org

Abstract—In this paper, we propose a real-time, non-destructive, and low-cost wheat mildew detection system using commodity WiFi devices, which is a new application of the Internet of Things (IoT) to agriculture applications. We first introduce wheat mildew and validate the feasibility of wheat mildew detection using WiFi Channel State Information (CSI) amplitude data. We then present the MiFi system design, including CSI sensing, preprocessing, radial basis function (RBF) neural network based detection modeling, and mildew detection. Our experimental results validate the effectiveness of the proposed MiFi system. The average detection accuracy of the MiFi system is over 90% under both line-of-sight (LOS) and non-line-of-sign (NLOS) scenarios.

Index Terms—Channel State Information (CSI); Commodity WiFi; Wheat Mildew Detection; Radial Basis Function (RBF); Machine Learning.

#### I. INTRODUCTION

With the rapid development of the world's population and the improvement of people's quality of life, the requirements for the quality and quantity of food (e.g., grain/wheat) are becoming more and more strict, and the demands are increasing rapidly every year [1]. The annual harvest of world food has exceeded 2 billion tons [2]. However, wheat mildew causes great loss of wheat processing quality and nutritional quality, and leads to even fungal contamination [3]. Due to the lack of professional knowledge and the high cost of testing equipment, many farmers and distributors cannot test the status of grain on a timely basis, and they can only judge whether the grain has mildew through experience. Rapid detection of mildew in grain can help farmers, distributors, and retailers to achieve more efficient and safer food storage, and thus to reduce food waste and cost.

It is a great challenge to detect mildew in grain quickly and at a low-cost. At present, detection of grain mildew mainly depends on manual detection. In fact, the degree of grain mildew is judged based on visual inspection and the olfactory experience of the inspector. The manual approach is time-consuming, error-prone, and not much helpful to quickly detect grain mildew. On the other hand, sensors or expensive instruments are also used for wheat mildew detection, such as electronic nose sensors [4] and near infrared spectroscopy [5]. However, the high cost of the required equipment prohibits their wide adoption.

WiFi has been a major wireless technology to provide communication service for mobile and wireless devices. The WiFi physical layer (PHY) incorporates Orthogonal Frequency-Division Multiplexing (OFDM) to address wireless propagation impairments such as frequency selective fading. For some commercial WiFi network interface cards (NIC), open-source device drivers are available to allow extraction of channel state information (CSI) of the OFDM PHY. For example, the Atheros 9kth NIC [6] can provide 56 subcarriers over a 20 MHz band for each received packet. Compared with received signal strength (RSS), CSI represents fine-grained channel information, which captures the wireless channel features that the packet experienced during propagation, such as the multipath effect, attenuation, and signal distortion. CSI amplitude and calibrated phase information are relatively stable over time, and have thus been employed for different wireless sensing purposes [7], such as vital sign monitoring [8], and indoor fingerprinting [9].

Motivated with the existing WiFi CSI-based sensing techniques, we propose WiFi CSI based wheat mildew detection, aiming to provide a low-cost, contact-free, and long-term mildew monitoring system. Wheat mildew involves a range of physiological changes of external and internal wheat status. When a WiFi signal passes through the wheat, changes in the mildew status of the wheat will cause significant and measurable variations of the WiFi signal, as recorded in the CSI values. In this paper, we experimentally verify the feasibility of wheat mildew detection using fine-grained CSI amplitude information, where CSI values are collected to detect three states of mildew, i.e., normal, initial stage of mildew, and complete mildew. We find that the CSI amplitude changes slightly when the wheat changes from the normal state to the early stage of mildew. However, the CSI amplitude data will be quite different when the wheat is completely mildewed.

In particular, we design the MiFi system, a device-free wheat **Mi**ldew detection system using WiFi CSI amplitude information. The MiFi system includes a sensing module, a preprocessing module, a detection modeling module, and a mildew detection module. The sensing module is to collect CSI amplitude data. The preprocessing module includes a Hampel identifier, environmental noise removal, subcarrier selection, and normalization. Specifically, we first apply a Hampel identifier to eliminate outliers from the collected

original CSI amplitude data. Then, a Butterworth filter is used to eliminate the ambient noise. The subcarrier that is most sensitive to CSI amplitude is selected using a mean absolute deviation method, and the corresponding CSI amplitude data is then normalized. In the detection modeling module, a *Radial Basis Function (RBF) neural network* is employed to detect wheat mildew based on calibrated CSI amplitude data, where *K*-means clustering is used to choose the parameters in the RBF neural network. Finally, in the detection module, we determine the wheat mildew state using a *classification matrix* through a combination of linear (i.e., the output layer) and non-linear (i.e., the Gaussian kernel) RBF neural networks.

The main contributions of this paper are summarized below.

- We verify the feasibility of using WiFi CSI amplitude information for wheat mildew detection. To the best of our knowledge, this is the first work that uses WiFi based RF sensing for wheat mildew detection.
- We design the MiFi system, which includes (i) a sensing module to collect CSI data; (ii) a preprocessing module to calibrate CSI amplitude data; (iii) a detection modeling module with a novel RBF based machine learning method; and (iv) a mildew detection module.
- We prototype the MiFi system with two commodity WiFi devices. The experimental results show that the proposed MiFi system can achieve an accuracy of over 90% on wheat mildew detection under both line-of-sight (LOS) and non-line-of-sign (NLOS) scenarios.

The remainder of this paper is organized as follows. The preliminaries and a feasibility study are presented in Section II. We introduce the MiFi system design in Section III and evaluate its performance in Section IV. Section V concludes this paper.

#### II. PRELIMINARIES AND FEASIBILITY STUDY

#### A. Wheat Mildew

Wheat mildew can lead to pollution of stored grain, loss of nutrients, and food-borne diseases in humans. The main causes of wheat mildew include microbial and environmental factors. Mildew is usually caused by the microbes in wheat granules during harvesting and by the granary microorganisms during storage [10]. On the other hand, wheat mildew is also affected by granary type, temperature, humidity, and other environmental factors [11]. In the early stage of wheat mildew, if timely measures are taken, the wheat will still be of use value. When the wheat has been completely mildewed, it will lose the use value and should be destroyed as soon as possible to avoid causing human diseases. A real-time, non-destructive, and low-cost wheat mildew detection system can be highly useful to ensure high safety of wheat storage.

The MiFi system design utilizes WiFi signals to monitor the mildew status of stored wheat with commodity WiFi devices. By analyzing the received WiFi signals after passing through stored wheat, e.g., with respect to CSI such as shadowing fading, reflection, and small-scale fading, the change of wheat mildew status can be detected. To quantify the effect, we

propose to use the concept of *dielectric constant* to indicate the change of wheat mildew states. The complex relative permittivity  $\varepsilon^*$  of a material in the frequency domain can be described as follows [12]

$$\varepsilon^* = \varepsilon' - j\varepsilon'',\tag{1}$$

where the real part  $\varepsilon'$  is the dielectric constant, representing the ability of the material to store energy in the frequency domain of the electric field, and the imaginary part  $\varepsilon''$  is a dielectric loss factor, which usually indicates the ability of a material to consume electrical energy, thus affecting the attenuation and absorption of WiFi signals.

In [13], Nelson et al. validate that difference in the water content of grains causes changes in the dielectric constant and the loss factor, which can be used as an indicator for detection of moisture content in grains. In fact, the dielectric constant can be indirectly used to determine whether the grain is mildewed by the water content. However, it requires an expensive, specialized instrument to detect the dielectric constant [12], which hampers the wide deployment of this technique in agriculture applications. In this paper, we propose to use off-the-shelf WiFi devices to detect wheat mildew by collecting and analyzing WiFi CSI values. Specifically, as WiFi signal passes through wheat, the electric field strength will change with the distance to the wheat surface. This effect can be captured by the attenuation factor  $\alpha$  of the dielectric properties of grain, which is given by [12]:

$$\alpha = \frac{2\pi}{\lambda_0} \sqrt{\frac{\varepsilon'}{2} \left( \sqrt{1 + \left(\frac{\varepsilon''}{\varepsilon'}\right)^2} - 1 \right)},\tag{2}$$

where  $\lambda_0$  is the wavelength of the wireless signal.

The change of wheat status from normal, to initial stage of mildew, and to complete mildew, will lead to increase of wheat temperature, moisture, and humidity of the external environment. These will in turn affect the dielectric constant  $\varepsilon'$  and dielectric loss factor  $\varepsilon''$ . Following (2), the attenuation factor  $\alpha$  will also change (as a function of  $\varepsilon'$  and  $\varepsilon''$ ), which can influence the energy of the electric field. In fact, we find the energy of the electric field will be greatly affected by wheat mildew, compared to that of normal wheat.

To quantify such energy change, we can detect the mildew status of wheat by analyzing the WiFi CSI amplitude information. With this approach, there is no need for expensive equipment to measure the dielectric constant, except for lowcost WiFi devices, for effective wheat mildew detection.

#### B. Channel State Information

Using some commodity NIC with open-source device drivers, CSI samples can be collected from  $N_s$  subcarriers, while each sample including the amplitude and phase of the subcarrier. The collected raw data includes the number of transmitting antennas  $N_{tx}$ , the number of receiving antennas  $N_{rx}$ , the packet transmission frequency f, and CSI data  $\mathbf{H}$ .

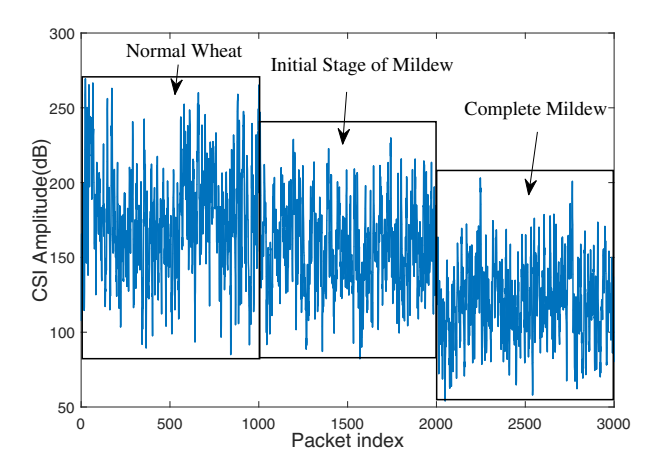


Fig. 1. CSI raw amplitude values collected from the same wheat pile going through the three states of mildew.

CSI data **H** is an  $N_{tx} \times N_{rx} \times N_s$  tensor, given by

$$\mathbf{H} = (H_{ijk})_{N_{tr} \times N_{rr} \times N_s}.$$
 (3)

In MiFi, 56 subcarriers are collected for the 20 MHz WiFi channel using an Atheros AR5BHB NIC. The kth subcarrier in  $\mathbf{H}$  for a given transmitting and receiving antenna pair can be characterized as

$$H_k = |H_k| \cdot \exp\{j \angle H_k\},\tag{4}$$

where  $|H_k|$  is the amplitude and  $\angle H_k$  is the phase.

#### C. Feasibility Study

This work is different from our previous work on WiFi based wheat moisture detection [14], [15], because wheat mildew will not only change the moisture, but also the temperature and air humidity of the entire wheat environment, which in turn influences the electric field. In our experiments, we find that wheat mildew affects the propagation of WiFi signals. To experimentally verify the feasibility of wheat mildew detection using fine-grained CSI data, we collect CSI amplitude data for the same pile of wheat (and the same locations for the wheat pile and WiFi devices) that develops mildew through the three states. Fig. 1 presents the collected CSI data from the three states, including normal, initial stage of mildew, and complete mildew. It can be seen that the CSI amplitude only changes slightly when the wheat state changes from normal to an early stage of mildew. However, the CSI amplitude data is obviously different when the wheat is completely mildewed. Thus, we conclude that CSI amplitude data can be utilized for wheat mildew detection.

# III. THE MIFI SYSTEM DESIGN

This section presents the MiFi system design. The system architecture, as shown in Fig. 2, includes four modules: (i) sensing, (ii) preprocessing, (iii) detection modeling, and (iv) mildew detection. First, in the CSI data sensing stage, we extract CSI amplitude data of the WiFi channel using an Atheros AR5BHB NIC. For data preprocessing, we develop a Hampel identifier to eliminate outliers, a Butterworth filter

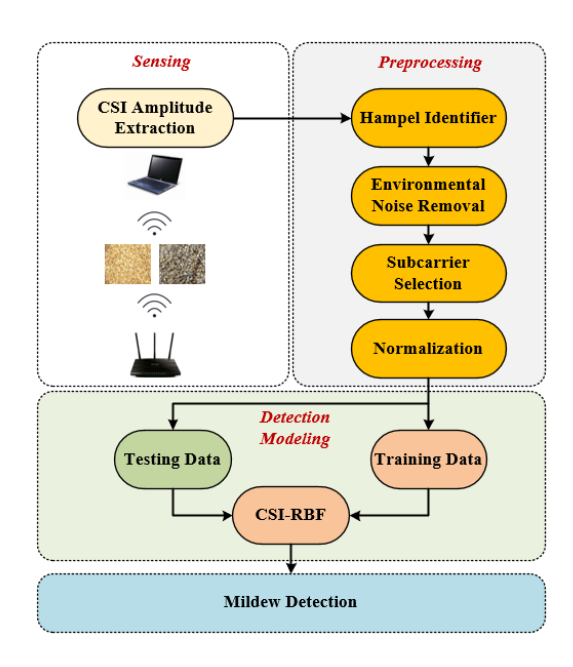


Fig. 2. The system architecture of MiFi.

to remove environment noise, a subcarrier selection procedure, and a normalization procedure. The third module is the CSI-RBF detection model. We divide the collected data into training data and testing data to establish and test the trained model. Finally, we obtain detection result of wheat mildew based on the CSI-RBF detection model.

#### A. CSI Amplitude Data Extraction

In the CSI data sensing stage, we use the Atheros AR5BHB NIC to collect CSI data from 56 subcarriers. For the normal wheat condition, we collect CSI data directly by WiFi packet transmissions through the wheat pile. For the initial stage of mildew and complete mildew conditions, we need to first culture mildew in the wheat examples. To accelerate the wheat mildew development, we use a chamber with temperature and humidity control capability: the temperature is maintained at 30°C and the air humidity is kept at 90%. After 2-3 days, the wheat begins to develop mildew and samples of the initial stage of mildew are collected. Complete mildew samples were obtained on the 8th day, and the CSI data is collected with the mildewed wheat. This way, we collect three types of CSI amplitude data, one for each mildew stages.

#### B. Hampel Identifier

In the data sensing module, some CSI data outliers will also be collected. For example, see Fig. 3 for the CSI amplitude data collected from the 20th subcarrier, where many high peaks and low valleys can be seen. These peaks are the outliers to be removed. In MiFi, we use a Hampel filter to detect and remove values that are significantly different from that in the normal CSI amplitude sequence.

Specifically, we apply a Hampel filter with a sliding window on each subcarrier to eliminate outliers. An N-sample CSI amplitude sequence from a subcarrier is denoted by

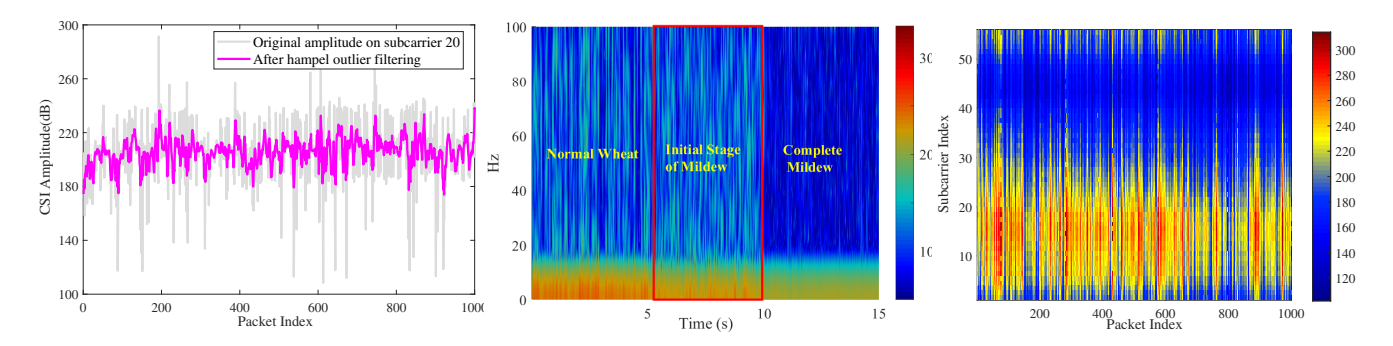


Fig. 3. Illustration of calibrating the CSI data Fig. 4. Spectrum of the CSI data from 20th Fig. 5. CSI amplitude for each subcarrier after collected from the 20th subcarrier. subcarrier for the three mildew states.

 $(X_1, X_2, ..., X_N)$ , where  $X_i$  is the *i*th sample of CSI amplitude from the subcarrier. Let X' be the median value in the CSI amplitude sequence. The Hampel identifier classifies a data point  $X_i$  as an abnormal value, if it deviates from the median absolute difference (MAD) by a predefined threshold:

$$\begin{cases} |X_i - X'| > l \cdot R, & \text{outlier} \\ |X_i - X'| \le l \cdot R, & \text{normal}, \end{cases} \quad i = 1, 2, ..., N, \quad (5)$$

where l is the predefined threshold and R is the MAD, defined as follows:

$$R = 1.4286 \cdot \text{median} \{ |X_i - X'|, i = 1, 2, ..., N \}.$$
 (6)

The constant 1.4286 ensures that the expected value of R is equal to the standard deviation of the normally distributed data [16]. In Fig. 3, we also plot the calibrated CSI amplitude data from the 20th subcarrier after Hampel filtering. It can be seen that the outliers are effectively removed.

#### C. Environmental Noise Removal

The calibrated CSI data still contains environment noise. After removing the outliers, we still need to reduce the environmental noise, to achieve a high detection accuracy. Fig. 4 shows the spectrum of the CSI data from the 20th subcarrier for the three mildew states. We observe that the frequency variation caused by mildew wheat over a period of time ranges from 0 Hz to 30 Hz. We thus apply a Butterworth filter to suppress the noises in other frequencies, including the environmental noise. The Butterworth filter utilizes a Butterworth function to approximate the system function of the filter, which is defined by the amplitude-frequency characteristics in the pass-band. The low-pass mode squared function of the Butterworth filter is given by

$$|L(f)|^2 = \left(1 + (f/f_c)^{2m}\right)^{-1},$$
 (7)

where m is the order of the filter and  $f_c$  is the cutoff frequency. In MiFi, the m value is 4 and the cutoff frequency is 30 Hz.

#### D. Subcarrier Selection

After the denoising procedure, the CSI amplitude has a variety of low frequency components, and exhibits different levels of sensitivity to mildew states of wheat. We use the mean absolute deviation of CSI amplitude data from every

subcarrier to measure the sensitivity of the subcarrier [8]. Generally, the larger the mean absolute deviation, the higher the sensitivity. It can be seen in Fig. 5 that the subcarriers with an index below 35 (among 56 subcarriers) are more sensitive (i.e., the red area in Fig. 5) and are more affected by wheat mildew. We thus choose CSI data from a more sensitive subcarrier with an index below 35 in MiFi.

#### E. Normalization

To speed up the computation of the model and improve the detection accuracy, we choose the zero-mean normalization method (i.e., Z-score normalization) to normalize the CSI amplitude data. The normalized data  $V_i$  is calculated by

$$V_i = \frac{1}{\sigma} \cdot (X_i - \bar{X}),\tag{8}$$

where  $\bar{X}$  and  $\sigma$  are the mean and standard deviation of the subcarrier's CSI amplitude data, respectively.

## F. CSI-RBF

After normalizing the CSI amplitude data, we apply the CSI-RBF neural network model to accurately recognize the different states of wheat mildew. In this section, we use the K-means algorithm to determine the hidden neuron parameters of the RBF kernel function.

1) K-means Clustering: K-means clustering is widely used in data clustering in many fields. It can be applied as an unsupervised learning to identify the parameter of a basis function and to determine the number of hidden neurons, which equals to the number of clusters. In our CSI-RBF model, we cluster CSI amplitude sequences based on a similarity score, which is calculated by the Euclidean distance between the amplitude data and the cluster mean. The Euclidean distance between two CSI amplitude sequences (in the form of two time series, each with size N) is given by

$$D(\mathbf{V}^1, \mathbf{V}^2) = \sqrt{(V_1^1 - V_1^2)^2 + \dots + (V_N^1 - V_N^2)^2}, \quad (9)$$

where  $V^1$  and  $V^2$  represent two CSI data streams.

2) CSI-RBF: RBF neural networks can overcome the short-comings of slow convergence and local minima, which has global approximation capabilities [17]. It can achieve a good performance in modeling nonlinear relationship with fast convergence characteristics. Motivated by the above advantages, we propose to employ RBF neural networks for rapid detection of wheat mildew.

Specifically, the MiFi system uses the RBF neural network as a classification algorithm. The basic structure of RBF consists of input neurons, hidden neurons, and output neurons. In MiFi, the input layer is clustered and the CSI amplitude matrix  $\mathbf{V} = (V_1, V_2, ..., V_N)$  is passed to F hidden neurons. The hidden layer can map network inputs in a non-linear manner, with each hidden neuron connected to each cluster center and width. Multiple activation functions can be applied to the hidden layer to maximize the accuracy of the output. We use the Gaussian function as follows:

$$\theta(v) = \exp\left\{-\left(\frac{v-\gamma}{\beta}\right)^2\right\},\tag{10}$$

where v,  $\gamma$ , and  $\beta$  are the predetermined input vectors, cluster center vectors, and hidden neuron widths by using K-means [17], respectively. Note that the number of hidden neurons is equal to the number of clusters.

The output layer uses a linear weighted sum function as output of the hidden layer. The m=3 wheat status categories can be recognized, and the linear function for the output layer is defined by:

$$Z_m = y_m(w, v) = \sum_{j=1}^{F} w_{jm} \cdot \theta_j(v) + b,$$
 (11)

where  $Z_m$  is the mth output neuron,  $w_{jm}$  is the weight from the jth hidden neuron to the mth output neuron,  $\theta_j(\cdot)$  is the Gaussian function in the hidden neuron, and b is the deviation. The CSI amplitude data collected from different mildew states is classified into m categories. The weights between the hidden layer and the output layer can be easily calculated with linear regression using the ordinary least squares (OLS) method.

# G. Mildew Detection

Finally, we compute the wheat mildew detection classification matrix through the combination of linear and non-linear RBF neural network models, as follows.

$$Z = [Z_1, Z_2, ..., Z_m], (12)$$

where m=3. In (12), the  $Z_1$  vector is the output regarded as normal wheat, the  $Z_2$  vector is the output regarded as early stage of mildew, and the  $Z_3$  vector is the output regarded as complete mildew.

# IV. IMPLEMENTATION, EXPERIMENTS AND DISCUSSIONS

#### A. Wheat Preparation

Fig. 6(a) and Fig. 6(b) show the normal wheat and the mildewed wheat, respectively. In Fig. 6(b), the wheat was taken from the constant temperature and humidity chamber on





(a) Normal wheat

(b) Mildewed wheat

Fig. 6. The wheat examples used in our experiments.





(a) The LOS scenario

(b) The NLOS scenario

Fig. 7. Experimental configuration for MiFi.

TABLE I EXPERIMENTAL WHEAT SAMPLE CONDITIONS

	Normal	Initial Stage of Mildew	Complete Mildew
Moisture	11.8%	12.9%	16.8%
Temperature	17°C	20°C	30°C
Internal air humidity	32%	48%	77%

the eighth day. For both figures, we measure the temperature and humidity inside the wheat samples. In addition, we use a standard drying method to measure the moisture content.

During the experiment, we take three different types of samples of wheat with the same weight to test their mildew conditions, including the normal wheat, the wheat in the initial stage of mildew, and the wheat with complete mildew. The water content, temperature, and humidity of the three different types of wheat samples are provided in Table I.

# B. Mi-Fi Implementation

The experimental hardware consists of two Dell PP181 laptops equipped with the Atheros AR5BHB NIC: one with a single antenna as transmitter and the other with three antennas as receiver. Both laptops run the kernel 4.1.10+ 32-bit Ubuntu Linux 14.04 operating system with 2 GB of RAM.

We conduct experiments in the Research Laboratory of Henan University of Technology, Zhengzhou, China. To test the effectiveness of our MiFi system, we considered both LOS and NLOS scenarios as shown in Fig. 7(a) and Fig. 7(b), respectively. For both experimental scenarios, we place the transmitter and receiver on both ends and different wheat samples in the middle for CSI data acquisition.

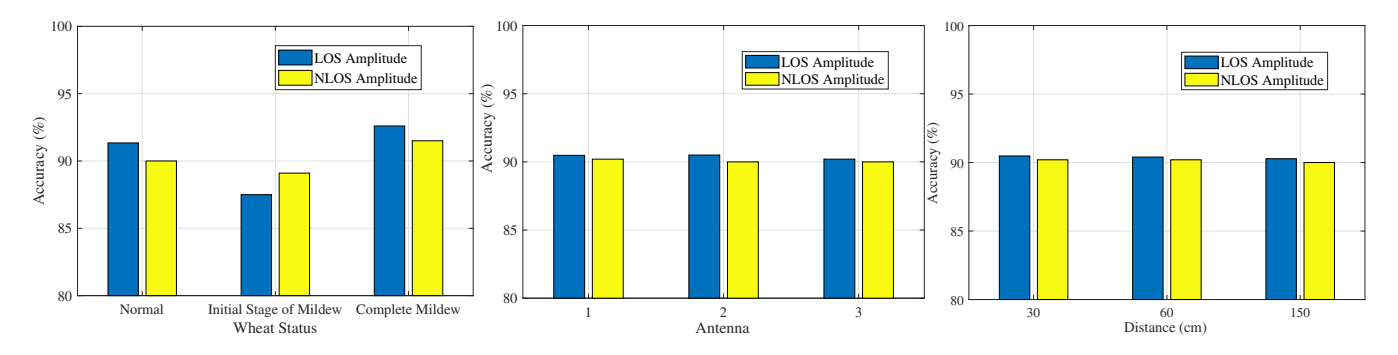


Fig. 8. Accuracy of wheat mildew detection under Fig. 9. Average detection accuracy for different Fig. 10. Average detection accuracy for different LOS and NLOS scenarios.

Average detection accuracy for different transmitter-receiver distances.

#### C. Experimental Results and Discussions

Fig. 8 shows the accuracy of wheat mildew detection in LOS and NLOS scenarios using CSI amplitude data. For the LOS scenario, we find that the MiFi system can achieve an over 90% detection accuracy when wheat is normal and completely mildewed. The detection accuracy of initial stage of mildew is less than 90% but still reaches 87.5%. The average accuracy under the LOS scene is 90.48%. For the NLOS scenario. the average accuracy achieved is 90.2%. Therefore, the proposed MiFi system can be sufficient for wheat mildew detection in both LOS and NLOS scenarios, because the impact of wheat mildew on WiFi signal propagation can be well captured by CSI amplitude data.

We next examine the impact of MiFi system configurations on detection accuracy. We focus on different antennas and different distances in this experiment. Fig. 9 shows the average detection accuracy using different antennas at the transmitter in both LOS and NLOS scenarios. The results show that the data of all the three antennas are effective. The average detection accuracies for the two scenarios are both above 90%. Fig. 10 shows the average detection accuracy for different distances between the transmitter and receiver in both LOS and NLOS scenarios. It can be seen that for different transmitter-receiver distances ranging from 30 cm to 150 cm, the detection accuracy of the MiFi system is always higher than 90%.

### V. Conclusions

In this paper, we presented MiFi, a low-cost and non-destructive wheat mildew detection system based on WiFi signals. We demonstrated the feasibility of wheat mildew detection using CSI amplitude data, and then presented the MiFi system design, with CSI data acquisition, data preprocessing, CSI-RBF detection modeling, and mildew detection. Our experimental results demonstrated the effectiveness of MiFi, which achieved an average accuracy over 90% under both LOS and NLOS scenarios.

#### **ACKNOWLEDGMENT**

This work is supported in part by the National Key Research and Development Program of China (2017YFD0401001), the Program for Science & Technology Innovation Talents in Universities of Henan Province (19HASTIT027), the NSFC (61772173), and the NSF under Grant CNS-1702957.

#### REFERENCES

- [1] D. Vasisht, Z. Kapetanovic, J. Won, X. Jin, R. Chandra, S. Sinha, A. Kapoor, M. Sudarshan, and S. Stratman, "Farmbeats: An IoT platform for data-driven agriculture," in *Proc. USENIX NSDI 2017*, Boston, MA, Mar. 2017, pp. 515–529.
- [2] D. S. Jayas, "Storing grains for food security and sustainability," Springer Agricultural Research, vol. 1, no. 1, pp. 21–24, 2012.
- [3] C. Lanier, E. Richard, N. Heutte, R. Picquet, V. Bouchart, and D. Garon, "Airborne molds and mycotoxins associated with handling of corn silage and oilseed cakes in agricultural environment," *Elsevier Atmospheric Environment*, vol. 44, no. 16, pp. 1980–1986, May 2010.
- [4] H. Zhang, J. Wang, S. Ye *et al.*, "Optimized of sensor array and detection of moldy degree for grain by electronic nose," *Chinese Journal of Sensors and Actuators*, vol. 20, no. 6, pp. 1207–1210, June 2007.
- [5] V. Fernández-Ibañez, A. Soldado, A. Martínez-Fernández, and B. De la Roza-Delgado, "Application of near infrared spectroscopy for rapid detection of aflatoxin B1 in maize and barley as analytical quality assessment," *Elsevier Food Chemistry*, vol. 113, no. 2, pp. 629–634, Mar. 2009.
- [6] Y. Xie, Z. Li, and M. Li, "Precise power delay profiling with commodity Wi-Fi," *IEEE Trans. Mobile Comput.*, to appear.
- [7] X. Wang, X. Wang, and S. Mao, "Rf sensing in the internet of things: A general deep learning framework," *IEEE Communications Magazine*, vol. 56, no. 9, pp. 62–67, 2018.
- [8] X. Wang, C. Yang, and S. Mao, "PhaseBeat: Exploiting CSI phase data for vital sign monitoring with commodity WiFi devices," in *Proc. IEEE ICDCS* 2017, Atlanta, GA, June 2017, pp. 1230–1239.
- [9] X. Wang, L. Gao, S. Mao, and S. Pandey, "CSI-based fingerprinting for indoor localization: A deep learning approach," *IEEE Trans. Veh. Technol.*, vol. 66, no. 1, pp. 763–776, Jan. 2017.
- [10] N. Magan and D. Aldred, "Post-harvest control strategies: minimizing mycotoxins in the food chain," *Elsevier Int. J. Food Microbiology*, vol. 119, no. 1-2, pp. 131–139, Oct. 2007.
- [11] U. Nithya, V. Chelladurai, D. Jayas, and N. White, "Safe storage guidelines for durum wheat," *Elsevier J. Stored Products Research*, vol. 47, no. 4, pp. 328–333, Oct. 2011.
- [12] V. Komarov, S. Wang, and J. Tang, "Permittivity and measurements," in *Encyclopedia of RF and Microwave Engineering*, K. Chang, Ed. Hoboken, NJ: John Wiley & Sons, 2005.
- [13] S. O. Nelson, S. Trabelsi, and A. W. Kraszewski, "Principles of microwave moisture measurement in grain," in *Proc. IEEE IMTC* 2002, Anchorage, AK, May 2002, pp. 99–102.
- [14] W. Yang, X. Wang, A. Song, and S. Mao, "Wi-Wheat: Contact-free wheat moisture detection using commodity WiFi," in *Proc. IEEE ICC* 2018, Kansas City, MO, May 2018, pp. 1–6.
- [15] W. Yang, X. Wang, S. Cao, H. Wang, and S. Mao, "Multi-class wheat moisture detection with 5GHz Wi-Fi: A deep LSTM approach," in *Proc. ICCCN 2018*, Hangzhou, China, July/Aug. 2018, pp. 1–9.
- [16] R. K. Pearson, "Outliers in process modeling and identification," *IEEE Trans. Control Syst. Technol.*, vol. 10, no. 1, pp. 55–63, Jan. 2002.
- [17] R. A. Johnson, D. W. Wichern et al., Applied Multivariate Statistical Analysis. Upper Saddle River, NJ: Prentice Hall, 2002.